



CHORUS

This is the accepted manuscript made available via CHORUS. The article has been published as:

Probing phase coherence in solid helium using torsional oscillators of different path lengths

Duk Y. Kim, Joshua T. West, Tyler A. Engstrom, Norbert Mulders, and Moses H. W. Chan
Phys. Rev. B **85**, 024533 — Published 24 January 2012

DOI: [10.1103/PhysRevB.85.024533](https://doi.org/10.1103/PhysRevB.85.024533)

Probing phase coherence in solid helium using torsional oscillators of different path lengths

Duk Y. Kim,^{1,*} Joshua T. West,¹ Tyler A. Engstrom,¹ Norbert Mulders,² and Moses H. W. Chan¹

¹*Department of Physics, The Pennsylvania State University, University Park, PA 16802, USA*

²*Department of Physics and Astronomy, University of Delaware, Newark, DE 19716, USA*

(Dated: January 10, 2012)

Long range phase coherence is a critical signature of macroscopic quantum phenomena. To date, non-classical rotational inertia (NCRI) of solid helium has been reported only in samples with physical dimension of at most five centimeters. We have investigated solid helium in longer path length torsional oscillators. Samples of length ranging from 6 to 100 cm were grown inside toroids and in self-connected long capillaries. NCRI of 4×10^{-5} and 3×10^{-5} were found in cells with path length of 6 and 9 cm. In cells with path length of 30 and 100 cm, NCRI if exists, is less than 7×10^{-5} and 4×10^{-5} respectively.

PACS numbers: 67.80.bd, 67.80.B-, 67.80.de

I. INTRODUCTION

Evidence of non-classical, i.e. missing, rotational inertia (NCRI) in solid helium at low temperature has been reported in torsional oscillator (TO) experiments in at least 9 different laboratories.^{1–11} The solid helium samples inside the TOs have dimensions of at most five centimeters. If solid helium at low temperature is a ‘standard’ superfluid, like superconductivity and superfluidity in liquid helium, one would expect the observation of NCRI will not be limited to centimeter length scales. In this paper we report a systematic search for NCRI in solid samples with path lengths of 6, 9, 30 and 100 cm. The 30 and 100 cm oscillators were made by winding capillaries onto bobbins like superconducting wires in a superconducting magnet in the persistent ready mode. Helium enters the cell through the fill line on the top and splits to a T-shaped junction secured at the top of the bobbin. From one end of the T, the capillary is wound down the side of the bobbin and then it is wound up along a second layer to the top and connected back to the same end of the T. The 6 and 9 cm oscillators were made by bending stainless steel tubes into the shape of a toroid. Measurements were carried out sequentially and all four oscillators used the same torsion rod and electrode assembly (Fig. 1). The solid helium samples were grown inside the capillaries and tubes using the block capillary method.

An important challenge facing the interpretation of TO results is the observation of an increase of up to 20% in the shear modulus of solid helium that tracks NCRI with identical temperature and ³He concentration dependences.¹² An increase in the shear modulus of solid helium stiffens the TO and causes the resonant period to drop thus mimicking NCRI.¹³ It is crucial to understand the causal relation and to separate the contribution of the shear modulus effect from NCRI. This shear modulus effect was calculated analytically by Maris and Balibar.¹⁴ For an ‘infinitely’ rigid TO oscillating at 1 kHz and containing an isotropic solid helium sample in the shape of

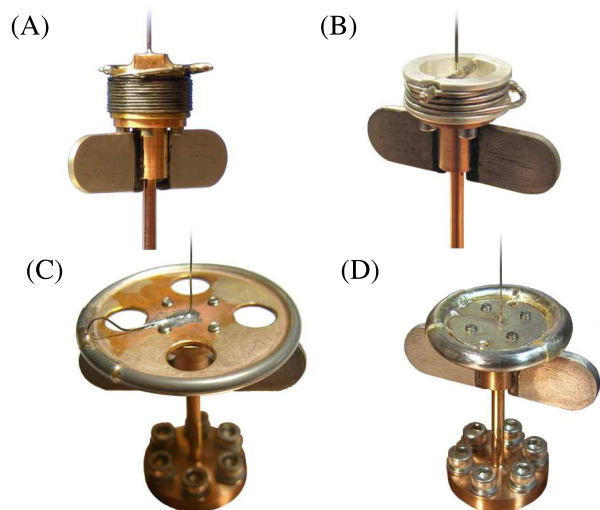


FIG. 1. (Color online) Torsional oscillators with (A) 100, (B) 30, (C) 9 and (D) 6 cm path length. The resonant frequencies are 842, 723, 570 and 750 Hz respectively. The IDs of the sample space are 0.4, 0.5, 1.8 and 2.7 mm.

a cylindrical disk of 1 cm in diameter and height, a 20% increase of the shear modulus of helium results in an apparent NCRI of approximately 1×10^{-4} . For TOs with a more complicated geometry, this shear modulus effect can be calculated more easily numerically by the finite element method (FEM).¹⁵ When we carried out a FEM simulation on a TO with the same parameters as those of Maris and Balibar, consistent results were found. The TOs used in this experiment are particularly amenable for reliable calculation of the shear modulus effect. The reason is that compared with ‘standard’ TOs that are typically glued together with epoxy, our cells are rigidly assembled with small amount of silver solder.

II. EXPERIMENTAL RESULTS

In this experiment, the TOs are kept oscillating at the resonant period by applying a constant ac voltage to one of the electrodes. Operating under this constant drive mode, the mechanical Q of a TO is proportional to and can be calculated from the amplitude of oscillation or the rim speed of the TO. In all the temperature scans measured in this experiment with the four TOs with different path lengths with and without helium samples, the mechanical Q 's are essentially temperature independent above 0.1 K but show a significant increase below 0.05 K. The resonant periods also show an abrupt upturn under high driving voltage (and high amplitude oscillation) in the same low temperature limit. This is commonly seen in many TOs and is most likely due to the material property of the beryllium copper torsion rod. No signature of a dissipation peak, i.e. a local minimum in the Q of the TO, correlated to the appearance of NCRI was found in any samples studied in this paper. This may be due to the very small NCRI found in this experiment. The Q of an empty cell is usually higher than that with a solid sample. However, this is not the case with the 100 cm path length cell and the 30 cm cell with aerogel (Fig. 3B). We do not have a clear explanation for this unusual behavior.

Figure 2 shows the resonant period and mechanical Q of the 100 cm path length TO with a 50 bar solid helium sample. Data are shown with the rim speeds of the TO, i.e. the capillary loop, oscillating at speeds of 1.3, 7.0 and 30 $\mu\text{m/s}$. In this paper, the reported rim speeds for all the measurements are measured at 0.5 K. The data of the empty cell at a rim speed of 20 $\mu\text{m/s}$ are also shown. When the period vs. temperature results of the solid sample are compared against the empty cell results, there is no sign of any period drop within the resolution of our period determination of 0.1 ns. Since the mass loading is 2600 ns, hence if NCRI is present, it is less than $0.1/2600$ or 4×10^{-5} . FEM simulations found the expected drop in period due to a 20% increase in shear modulus to be 10^{-3} ns, two orders of magnitude smaller than the resolution of the period measurement. Since the sample cross section is narrow, the expected shear modulus effect is much smaller than that found by Maris and Balibar for a solid sample with linear dimension of 1 cm.

While the 100 cm oscillator consists of 25 windings of CuNi capillary, the 30 cm path length oscillator has 7 turns of Ni capillary. Figure 3A shows the resonant period and the mechanical Q of the TO with a 45 bar solid helium sample. The scatter of the data is approximately 0.1 ns. Within this uncertainty, the periods at the three different rim speeds show consistent temperature dependence with no measurable decrease at low temperatures when compared against the empty cell background. A total of five solid samples with different pressures were studied. Three samples (35, 40, 45 bar) were made with ^4He of natural isotopic purity, with 0.3 parts per mil-

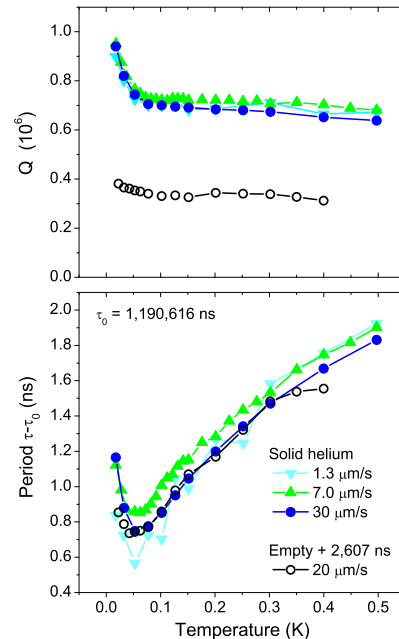


FIG. 2. (Color online) The resonant period and the mechanical Q of the 100 cm torsional oscillator as a function of temperature. The period is shifted by an amount τ_0 (shown in the figure) for easy display. The period of the empty oscillator is further shifted to account for mass loading of 2607 ns. We note that the period readings at different rim velocities are not shifted with respect to each other. The rim velocities are measured at 0.5 K.

lion (ppm) ^3He , and the other two samples contain 2.5 ppm ^3He (45 bar) and 20 ppm ^3He (50 bar). We did not observe period decrease larger than 0.1 ns at low temperature in any of these samples. This means that if present, the NCRI fraction is smaller than 7×10^{-5} . The expected period drop due to the shear modulus increase was calculated by FEM to be comparable with the 100 cm cell.

We fabricated two identical TOs with path length of 30 cm and grew silica aerogel of 95% porosity in one of the cells. The resonant period of the aerogel cell is slightly larger (1.39 vs. 1.38 ms) and the mass loading due to a 45 bar solid sample is slightly smaller than the cell without aerogel, consistent with expectation. The solid helium sample in aerogel shows no period drop larger than 0.2 ns and no NCRI larger than 1.4×10^{-4} (Fig. 3B). The disorder induced by the heterogeneous silica strands in aerogel did not significantly enhance NCRI in the solid. This is consistent with the recent findings in conventional TOs where the NCRI of solid ^4He in aerogel was found to be comparable to samples grown from superfluid.¹⁶ A liquid helium sample of 1.5 bar was also studied. With the help of aerogel entraining the normal fluid, the superfluid fraction can be measured. A sharp superfluid transition was found and the total period drop at low temperature was 84% of the mass loading due to normal liquid. Such a decoupling is reasonable considering the tortuosity of

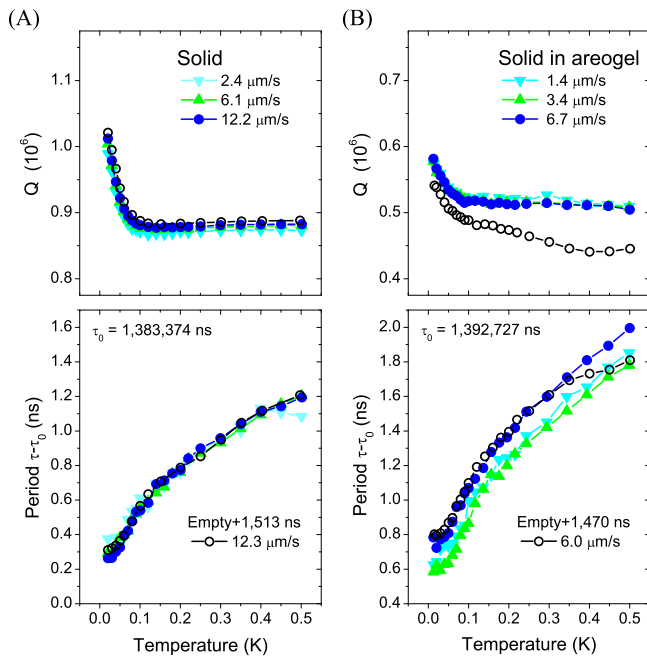


FIG. 3. (Color online) The resonant period and the mechanical Q of the 30 cm torsional oscillators containing (A) 45 bar solid helium and (B) 45 bar solid helium inside aerogel.

the aerogel and the immobile inert layer on the aerogel surface. In all other TOs of this paper without aerogel, signatures in periods and mechanical Q's were seen at the superfluid transition.

Figure 4 shows the resonant period and the mechanical Q of the 9 cm TO with solid samples at 41 and 48 bar. The mass loadings of the two samples were found to be 15,013 and 15,221 ns in excellent agreement with that found by FEM (15,100 and 15,348 ns). The period data of both samples show a small drop (as compared against the empty cell curve) below 100 mK. For the 48 bar sample the total period drops at the minimum temperature are 0.60 and 0.36 ns respectively for rim speeds of 4.5 and 22 $\mu\text{m/s}$. Period drops of 0.35, 0.29 and 0.21 ns are found for the quench-cooled 41 bar sample at rim speeds of 4.5, 22.8 and 112 $\mu\text{m/s}$. The average period drop of the two samples at low speeds is 0.47 (± 0.1) ns, equivalent to a NCRI fraction of $3 \pm 0.7 \times 10^{-5}$. Our FEM simulation found a resonant period drop of 0.08 ns for a 20% increase in the shear modulus of solid helium. This is on the order of the scatter of the period readings and 20% is the maximum value we can expect in a polycrystalline solid. Our attempt to introduce disorder by quench-cooling the 41 bar sample did not enhance NCRI.

Figure 5 shows the resonant period and the mechanical Q of the 6 cm TO with four solid samples. Three samples (30 bar, 50 bar and another 50 bar quench-cooled sample) were grown from ^4He with 0.3 ppm ^3He . The other 50 bar sample is enriched with 10 ppm ^3He . The mass loading of the 30 and 50 bar samples were found to be 12,642 and 13,695 ns, again in excellent agreement

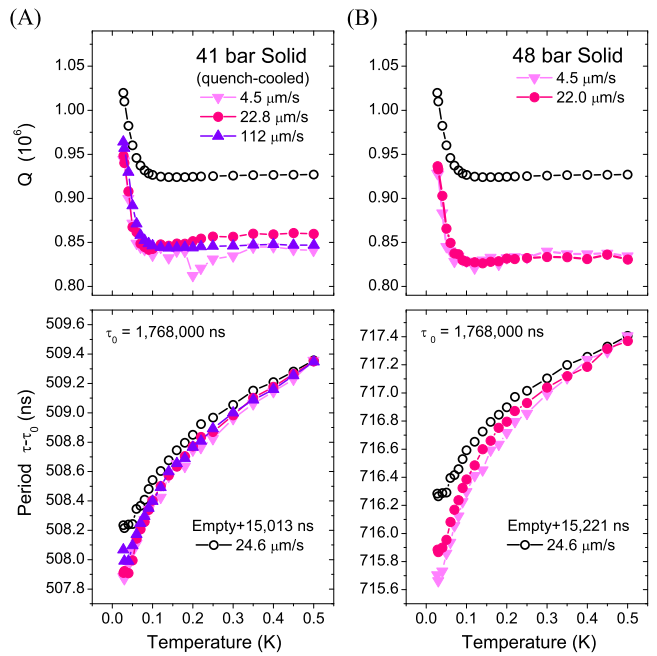


FIG. 4. (Color online) The resonant period and the mechanical Q of the 9 cm torsional oscillator containing (A) 41 bar quench-cooled and (B) 48 bar solid helium. The period data with the rim velocity of 22.8 $\mu\text{m/s}$ (A) is shifted down by 0.15 ns and 22.0 $\mu\text{m/s}$ (B) is shifted up by 0.15 ns for easy comparison.

with the FEM values of 13,020 and 13,776 ns. Clear period drops are seen in the three 0.3 ppm samples below 150 mK. The low temperature period drops at low rim speeds (5.8~11.9 $\mu\text{m/s}$) were found to be 0.50 (30 bar), 0.55 (50 bar) and 0.60 ns (50 bar quench-cooled). The period drops at high speeds (118~120 $\mu\text{m/s}$) were found to be the same as the low speed values within the scatter (0.1 ns). The average period drop for these three samples of $0.55 (\pm 0.1)$ ns correspond to a NCRI fraction of $4 \pm 0.7 \times 10^{-5}$. The period drop due to a 20% shear modulus increase was calculated by FEM to be 0.16 ns. The larger shear modulus effect found for the 6 cm cell as compared to the 9 cm cell is primarily due to the larger cross section (2.7 vs. 1.8 mm ID) of the solid ^4He sample. The period of the 10 ppm ^3He sample begins to deviate from the empty cell curve near 0.4 K instead of 0.15 K. The drop in period at low temperature is at most 0.26 ns. This behavior is consistent with prior experiments with ^3He enriched samples in conventional TOs.¹⁷

As mentioned above, there is no observable dissipation peak correlated with NCRI in our experiment with all four TOs. A broad minimum of the Q around 60 mK was found in the 30 bar sample (Fig. 5A) in the 6 cm TO. For the 50 bar samples, the minima are found near 1.3 K (Fig. 5B and Fig 5C). The exact origin of this broad Q minimum is not clear. In a recent experiment, Eyal and collaborators¹⁸ found a large drop in the period near 1.5 K. We extended the measurements for a few samples in

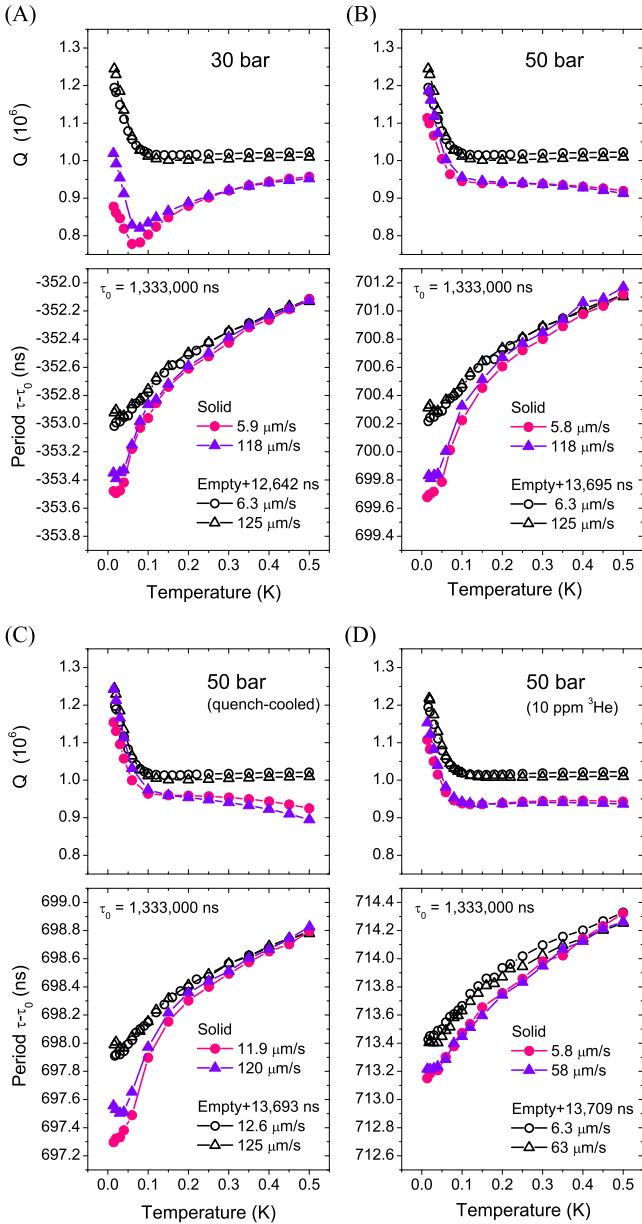


FIG. 5. (Color online) The resonant period and the mechanical Q of the 6 cm torsional oscillator. Panel (D) shows results for solid ^4He containing 10 ppm ^3He . All other samples are of natural isotopic purity (0.3 ppm ^3He).

the 6 and 9 cm TOs up to melting points. However, we could not find any period drop larger than the scatter of the data or 0.1 ns at temperatures higher than 0.5 K.

III. DISCUSSIONS

Since the observed period drops in the 6 and 9 cm TOs are only three to six times larger than that attributable to the shear modulus effect, one may wonder if it is possible that we have under-estimated the effect and there is no

need to invoke NCRI. It was found recently that in a single crystal the change in the shear modulus can be as high as 86%¹⁹ instead of between 1 to 20% as reported in polycrystalline samples.^{12,20} Therefore if we have single crystals in our TOs, then the observed period drops may be (solely) the consequence of the shear modulus effect. However all of the samples studied in this experiment were made by the block capillary method and two were quench-cooled as rapidly as possible, therefore it is very unlikely that the samples are single crystal. If we have polycrystalline samples, then it is difficult to ‘increase’ the magnitude of the shear modulus effect. This is the case because the FEM calculation is very straight forward considering the simplicity in both the geometry (toroidal) and the construction (consists only of the metal tube and the sample) of the TOs. Since the 30 and 100 cm cells are not able to resolve NCRI smaller than 7×10^{-5} and 4×10^{-5} , we are not able to conclude if NCRI is attenuated for lengths longer than 9 cm.

An interesting question raised by this experiment is how to understand the exceptionally small NCRI found in the 6 and 9 cm TOs in the light of the very large variation found in other TOs that ranges upward to 5×10^{-2} or even 2×10^{-1} .⁵ Since the ‘path lengths’ of many conventional TOs are already on the order of 4 cm, it is unlikely that the slightly longer length at 6 cm is responsible for dramatic (two orders of magnitude, from typical 10^{-2} or 10^{-3} to 4×10^{-5}) decrease in NCRI. Another possibility is that the toroidal geometry may be more amenable for the growth of higher quality crystalline samples which may result in smaller NCRI. However, evidence in support of disorder as the explanation for larger NCRI is at best inconclusive. As noted above, NCRI of solid ^4He did not show any enhancement when it is embedded in highly heterogeneous aerogel. A recent experiment also failed to find any correlation between NCRI and the thermal conductivity (hence crystallinity) of the sample.¹⁰

The modulus effect of solid ^4He can be greatly multiplied in a TO that is not completely rigid. A clear example is the TO used by Reppy.²¹ It resembles a concentric double torsion pendulum with an inner cylinder suspended from the outer body by a diaphragm. In such a configuration, the solid helium sample confined in the thin annulus engulfing the inner cylinder contributes to the mechanical coupling of the cylinder to the rest of the TO. This coupling is strengthened when the solid helium sample is stiffened at low temperature. This has the consequence of stiffening the TO and raise its resonant frequency. Since the annular helium space is particularly small, the drop in the resonant period mimics a mass decoupling of 5×10^{-2} . This scenario is consistent with his conclusion on the compound oscillator experiment that the most of the period drop is attributable to shear modulus stiffening.²² While Reppy’s TO is exceptionally ‘pendulous’, it does illustrate that the shear modulus effect coupled with TOs that are not completely rigid can give rise to a large but ‘false’ NCRI signal.¹⁴ The typical NCRI reported to date ranges between 10^{-3}

and 10^{-2} . However, NCRI of as small as 1.5×10^{-4} , 3×10^{-4} and 4×10^{-4} have been reported.^{16,23,24} We note that an early TO experiment at Bell Labs failed to detect NCRI signals above the 1×10^{-4} level for spherical samples of solid ^4He with varying degrees of ^3He concentration ranging from 0.3 to 411 ppm.²⁵ A recent experiment with a transparent sapphire TO found no evidence of NCRI in polycrystalline samples within their experimental resolution of 10^{-4} . Larger period drops, corresponding to possible NCRI of 10^{-3} , were found in single crystal samples.¹¹ However, the authors suggested that this larger period drop may be due to a larger shear modulus effect in single crystals.

If solid ^4He does have ‘real’ NCRI, it is difficult to see how our toroidal (or any other) TO will measure a value that is smaller than this true value. We showed that there are mechanisms (e.g. shear modulus effect) that may lead one to measure a NCRI that is larger than the intrinsic value. The results presented here therefore suggest that the real NCRI of solid ^4He may in fact be on the order of 3×10^{-5} . Recently, dc mass flow through solid ^4He was demonstrated by contacting the two ends of the solid sample with superfluid liquid.²⁶ If one assumes a critical velocity of $10 \mu\text{m/s}$, then the flow rate is consistent with a NCRI between 3×10^{-5} and 1.2×10^{-4} .

It has been proposed that the dislocation line is superfluid and NCRI is the consequence of such an interconnected dislocation network^{27,28} in the stiffened state. If the core diameter of a dislocation is taken to be 6 \AA ²⁷ and if we assume the largest dislocation density of 10^{10} cm^{-2} as reported in ultrasound studies²⁹ and if we further assume the dislocation lines are streamlined to give maximum superfluidity, then the expected NCRI of such a model is 3×10^{-5} . However the 10^{10} cm^{-2} number for dislocation density appears to be an outlier, more reliable numbers are on the order of 10^4 and 10^6 .³⁰ It should also be noted that this superfluid dislocation line network model for NCRI and the shear modulus stiffening that mimic NCRI are not applicable for solid helium embedded in porous Vycor glass and porous gold.^{1,8,31} In these experiments, NCRI fractions on the order of 10^{-2} were observed. There is another recent TO experiment that is difficult to reconcile with the very small NCRI presented here. Specifically, Choi and collaborators found that when their TO is subjected to dc rotation, the sizable NCRI (10^{-2}) was found to diminish with increasing dc rotation speed.³² It is difficult not to interpret this result as a consequence of the dc rotation effect on quantum vorticity and superfluidity.

ACKNOWLEDGMENTS

Support for this experiment was provided by NSF Grants No. DMR0706339 and DMR1103159. The idea of looking for NCRI in a sample of long path length originated during a conversation with John Reppy.

-
- * dukyng@gmail.com
- ¹ E. Kim and M. H. W. Chan, *Nature* **427**, 225 (2004).
 - ² E. Kim and M. H. W. Chan, *Science* **305**, 1941 (2004).
 - ³ M. Kondo, S. Takada, Y. Shibayama, and K. Shirahama, *J. Low Temp. Phys.* **148**, 695 (2007).
 - ⁴ Y. Aoki, J. C. Graves, and H. Kojima, *Phys. Rev. Lett.* **99**, 015301 (2007).
 - ⁵ A. S. C. Rittner and J. D. Reppy, *Phys. Rev. Lett.* **98**, 175302 (2007).
 - ⁶ A. Penzev, Y. Yasuta, and M. Kubota, *Phys. Rev. Lett.* **101**, 065301 (2008).
 - ⁷ B. Hunt, E. Pratt, V. Gadagkar, M. Yamashita, A. V. Balatsky, and J. C. Davis, *Science* **324**, 632 (2009).
 - ⁸ D. Y. Kim, S. Kwon, H. Choi, H. C. Kim, and E. Kim, *New Journal of Physics* **12**, 033004 (2010).
 - ⁹ R. Toda, P. Gumann, K. Kosaka, M. Kanemoto, W. Onoe, and Y. Sasaki, *Phys. Rev. B* **81**, 214515 (2010).
 - ¹⁰ D. E. Zmeev and A. I. Golov, *Phys. Rev. Lett.* **107**, 065302 (2011).
 - ¹¹ A. D. Fefferman, X. Rojas, A. Haziot, S. Balibar, J. T. West, and M. H. W. Chan, To be published.
 - ¹² J. Day and J. Beamish, *Nature* **450**, 853 (2007).
 - ¹³ I. Iwasa, *Phys. Rev. B* **81**, 104527 (2010).
 - ¹⁴ H. Maris and S. Balibar, *J. Low Temp. Phys.* **162**, 12 (2011).
 - ¹⁵ A. C. Clark, J. D. Maynard, and M. H. W. Chan, *Phys. Rev. B* **77**, 184513 (2008).
 - ¹⁶ N. Mulders, J. T. West, M. H. W. Chan, C. N. Kodituwakku, C. A. Burns, and L. B. Lurio, *Phys. Rev. Lett.* **101**, 165303 (2008).
 - ¹⁷ E. Kim, J. S. Xia, J. T. West, X. Lin, A. C. Clark, and M. H. W. Chan, *Phys. Rev. Lett.* **100**, 065301 (2008).
 - ¹⁸ A. Eyal, O. Pelleg, L. Embon, and E. Polturak, *Phys. Rev. Lett.* **105**, 025301 (2010).
 - ¹⁹ X. Rojas, A. Haziot, V. Bapst, S. Balibar, and H. J. Maris, *Phys. Rev. Lett.* **105**, 145302 (2010).
 - ²⁰ X. Rojas, Ph.D. thesis, Université Paris 6 (2011).
 - ²¹ J. D. Reppy, *Phys. Rev. Lett.* **104**, 255301 (2010).
 - ²² X. Mi, E. Mueller, and J. D. Reppy, arXiv:1109.6818v1.
 - ²³ J. T. West, O. Syshchenko, J. Beamish, and M. H. W. Chan, *Nature Physics* **5**, 598 (2009).
 - ²⁴ A. C. Clark, J. T. West, and M. H. W. Chan, *Phys. Rev. Lett.* **99**, 135302 (2007).
 - ²⁵ D. J. Bishop, M. A. Paalanen, and J. D. Reppy, *Phys. Rev. B* **24**, 2844 (1981).
 - ²⁶ M. W. Ray and R. B. Hallock, *Phys. Rev. B* **79**, 224302 (2009).
 - ²⁷ M. Boninsegni, A. B. Kuklov, L. Pollet, N. V. Prokof'ev, B. V. Svistunov, and M. Troyer, *Phys. Rev. Lett.* **99**, 035301 (2007).
 - ²⁸ L. Pollet, M. Boninsegni, A. B. Kuklov, N. V. Prokof'ev, B. V. Svistunov, and M. Troyer, *Phys. Rev. Lett.* **101**, 097202 (2008).
 - ²⁹ Y. Hiki and F. Tsuruoka, *Phys. Rev. B* **27**, 696 (1983).
 - ³⁰ R. Wanner, I. Iwasa, and S. Wales, *Solid State Communications* **18**, 853 (1976).
 - ³¹ E. Kim and M. H. W. Chan, *J. Low Temp. Phys.* **138**, 859 (2005).
 - ³² H. Choi, D. Takahashi, K. Kono, and E. Kim, *Science* **330**, 1512 (2010).